
Article:
Morgado, E, Parada, MA, Morgan, DJ orcid.org/0000-0002-7292-2536 et al. (3 more authors) (2017) Transient shallow reservoirs beneath small eruptive centres: Constraints from Mg-Fe interdiffusion in olivine. Journal of Volcanology and Geothermal Research, 347. pp. 327-336. ISSN 0377-0273

https://doi.org/10.1016/j.jvolgeores.2017.10.002

Transient shallow reservoirs beneath small eruptive centres: Constraints from Mg-Fe interdiffusion in olivine

E. Morgado, M.A. Parada, D.J. Morgan, F. Gutiérrez, A. Castruccio, C. Contreras

PII: S0377-0273(17)30031-8
DOI: doi:10.1016/j.jvolgeores.2017.10.002
Reference: VOLGEO 6210

To appear in: *Journal of Volcanology and Geothermal Research*

Received date: 13 January 2017
Revised date: 2 October 2017
Accepted date: 2 October 2017

Please cite this article as: E. Morgado, M.A. Parada, D.J. Morgan, F. Gutiérrez, A. Castruccio, C. Contreras , Transient shallow reservoirs beneath small eruptive centres: Constraints from Mg-Fe interdiffusion in olivine. The address for the corresponding author was captured as affiliation for all authors. Please check if appropriate. Volgeo(2017), doi:10.1016/j.jvolgeores.2017.10.002

TRANSIENT SHALLOW RESERVOIRS BENEATH SMALL ERUPTIVE CENTRES: CONSTRAINTS FROM Mg-Fe INTERDIFFUSION IN OLIVINE

Morgado, E.[1, 2*], Parada, M. A.[2], Morgan, D.J.[1], Gutiérrez, F.[2, 3], Castruccio, A.[2], Contreras, C.[2,a]

[1] Institute of Geophysics and Tectonics, School of Earth and Environment, University of Leeds, Leeds LS2 9JT, UK

[2] Departamento de Geología, Facultad de Ciencias Físicas y Matemáticas, Universidad de Chile, Chile/ Centro de Excelencia en Geotermia de los Andes (CEGA)

[3] Advanced Mining Technology Center, Universidad de Chile

[*] Corresponding author at: Institute of Geophysics and Tectonics, School of Earth and Environment, University of Leeds, Leeds LS2 9JT, UK and Centro de Excelencia de Geotermia de los Andes (CEGA), Departamento de Geología, Facultad de Ciencias Físicas y Matemáticas, Universidad de Chile, Santiago 8370450, Chile.

[a] Now at: School of Earth Sciences, Faculty of Science, University of Bristol, Bristol BS8 1RJ, UK

E-mail addresses: eeeem@leeds.ac.uk (E. Morgado), maparada@cec.uchile.cl (M. Parada), d.j.morgan@leeds.ac.uk (D. Morgan), franciscogutierrez@uchile.cl (F. Gutiérrez), acastruc@ing.uchile.cl (A. Castruccio), clcontre@ug.uchile.cl (C. Contreras).

Abstract

Small eruptive centres commonly have more primitive lavas than those associated with stratovolcanoes, an observation that has been taken to indicate a short magma residence in the crust relative to those reservoirs below stratovolcanoes. The Caburgua cones of the Andean Southern Volcanic Zone from a basaltic small eruptive centre where this can be tested/ Here, we use MELTS simulations, and the available thermobarometry data to determine the conditions of olivine crystal rim formation and the Mg-Fe diffusion modelling to determine the magma residence times of those rims in the crust. Results yield timescales varying from a few days to dozens of days, and if freezing is to be avoided, can only be explained by some

form of storage or slow transport through at least one shallow magma body. The longest durations of magma residence seen in the olivine rim zones are up to 471 days. These timescales are shorter than those estimated (decadal) from the nearby, more-differentiated, and well-established stratovolcano, Villarrica, which has a dominantly basaltic andesite composition. For Caburgua cones, we propose the existence of a transient reservoir, in contrast to a long-lived reservoir such as that inferred beneath the adjacent Villarrica stratovolcano.

1. Introduction

Small eruptive centres (SECs) are commonly found in clusters comprising volcanic fields, expressed as arrays of volcanic cones aligned along regional structures (e.g. López-Escobar et al., 1995a; Connor et al., 2000; Valentine and Perry, 2006). Although these cones may be composed of products of different compositions, they are commonly basaltic, though and the presence of primitive basalts is rare (Valentine and Gregg, 2008; McGee and Smith, 2016).

Magma input rates, related to the degree of melt interconnection through coalescing conduits, combined with the tectonic setting have been named as significant factors controlling the genesis of SECs relative to stratovolcanoes (e.g., Takada, 1990; Cañón-Tapia and Walker, 2004). Usually SECs are related to high deformation rates and low magma supply rates (e.g., Takada 1994a, 1994b). For developing a field of small eruptive centres, Németh (2010) determined that time-integrated magma fluxes of 0.01 km^3/yr or less are necessary and that these small-volume ascending magmas can be frozen within the crust over just a few days, if the rate of magma ascent is slower than that of solidification, or if the trajectory of ascending magma is too long for a given solidification rate (e.g., Auckland Volcanic Field, Smith et al., 2008, McGee et al., 2012). The main advantage of focusing on eruptions at SECs is that due to the implied rapid ascent, they are inferred to have had little opportunity for extensive

interaction with the upper crust, are not expected to be associated with shallow magma chambers, and may therefore represent more closely the mantle source and the ascent process itself (e.g. Lara et al., 2006; Cembrano and Lara, 2009; McGee and Smith, 2016).

Despite the expected simplicity of small eruptive centres, signs of more complex plumbing systems have been exceptionally recognized in SECs, in particular expressed as crystals evidencing polybaric crystallisation and longer magma residence times seen in erupted phenocrysts. For example, at Jorullo SEC (Mexico) a long-lived (~15 years, Luhr and Carmichael, 1985) eruption was studied by Johnson et al. (2008) via groundmass crystallinity, olivine-hosted melt inclusions and olivine diffusion modelling; multi-stage crystallisation processes (lower and upper crust) were recognized and relatively long magma residence times (in cases >1,000 days) in the upper crust suggested the presence of a shallow reservoir.

Unlike stratovolcanic settings, where complex mineral zonation and disequilibrium features are commonly recognized, the products of most SECs exhibit textural equilibrium features, and individual mineral grains possess very thin zonation at the crystal rims, if zonation is present at all (e.g., Cayutué-La Viguería group, López-Escobar et al., 1995a, b; Auckland Volcanic Field, Cook et al., 2005; Carrán-Los Venados volcanic field, Bucchi et al., 2015). Such differences between stratovolcanoes and SECs can be attributed to the action of numerous processes in stratovolcanoes, such as magma recharge, heating, mixing or the ascent of plumes within extended, long-lived magmatic reservoirs (e.g., Gutiérrez et al., 2005; Ginibre and Wörner, 2007; Ruprecht and Bachmann, 2010; Lohmar et al., 2012; Bouvet de Maisonneuve et al., 2012).

Magma ascent processes have been studied using different techniques and approaches such as: U-Th-Ra isotopic disequilibrium in magma (Condomines et al., 1988); seismicity during

eruptive periods (Scandone and Malone, 1985; Lees and Crosson, 1989; Endo et al., 1996); the presence of dense xenoliths carried to the surface by magma (e.g. Spera, 1984; Sparks et al., 2006); and reaction rim growth on amphibole phenocrysts (Rutherford and Hill, 1993). Another method used to constrain the timescales of the pre-eruptive processes is modelling element diffusion within and between crystals (e.g. Zellmer et al., 1999; Costa et al., 2003; 2008; 2013; Morgan et al., 2004; Costa and Dungan, 2005; Chamberlain et al., 2014; Shea et al., 2015; Hartley et al., 2016). Diffusional methods combined with calculations of magmatic intensive conditions (thermobarometry) allow the determination of a range of timescales from short-lived (e.g., minutes: Charlier et al., 2010; days: Costa and Dungan, 2005; Martin et al., 2008; Kahl et al., 2011) to long-lived (e.g. centuries: Morgan and Blake, 2006; Morgan et al., 2006) pre-eruptive processes, dependent on the mineral-element pair being studied. This study focuses on olivine residence times and magma ascent determined via Mg-Fe interdiffusion modelling of compositional profiles within olivine crystals from the Caburgua cones, a sub-division of the Caburgua-Huelemolle Small Eruptive Centres (CHSEC) in the Andean Southern Volcanic Zone (Fig.1). The sample material comprises crystals extracted from a volcanic bomb (details in sections 2 and 3); this ensures that samples will have been subjected to rapid quenching, removing the necessity to consider significant post-eruptive surface cooling, and ensuring that preserved profiles reflect partial re-equilibration at magmatic temperatures. Mg-Fe interdiffusion in olivine in magmatic systems typically yields timescales of days to few years (e.g., Hartley et al., 2016; Rae et al., 2016; Kahl et al., 2015; 2017), important for assessing magma ascent rates and the staging of magma prior to eruption due to high Mg-Fe diffusivity in comparison with other magmatic mineral phases (e.g., Müller et al., 2013). In some cases, calculated timescales (days to years) can be correlated with volcanic monitoring data (e.g., Kahl et al., 2011; 2013).

A regional example of a residence times and magma ascent rate study was the work of Lara et al. (2006) on the Carrán-Los Venados SECs and the adjacent Cordón Caulle-Puyehue stratovolcano complex. Cr-Rb data and fractional crystallisation modelling were used to show that the Carrán-Los Venados SECs are less-contaminated than magmas of the adjacent Cordón Caulle-Puyehue complex, inferring shorter crustal residence times at the SECs. Magma ascent at Cordón Caulle-Puyehue complex, by contrast, is suggested to have been rapid, from the result of uranium-series isotopes (Jicha et al., 2007). Parallel uranium-series work on magmas of the CHSEC by McGee et al. (2017) has suggested both fast melting and ascent of magmas after fluid addition to the mantle region beneath.

An investigation of thermobarometry (olivine-augite phenocryst pairs), combined with thermodynamic modelling (MELTS), allows the determination of magmatic conditions (P, T, X) for the formation of mineral zoning. Combined with study of subsequent diffusion processes, this can place a time constraint on crystal growth. This study aims to reveal the existence of any day- to month-scale pre-eruptive events, and therefore the possible existence of transient upper-crustal reservoirs beneath the Caburgua cones. By “transient”, in this context, we consider “transient reservoirs” to be those reservoirs where magma can be stored for periods ranging up to decadal timescales, in effect where magma injections into cool crust are too infrequent to sustain an effectively permanent magma body, but may be sufficient to support a series of eruptions over tens of years before the system freezes. More specifically, this study represents the first petrological estimation of magma ascent rates for a South American SEC system. The techniques used here could be successfully applied in other situations where short upper crustal residence occurs, in order to determine pressures and temperatures of storage and possible durations.

2. Geology, mineralogy and pre- and syn- eruptive conditions of the Caburgua cones

The Caburgua cones form the northwest extremity of the CHSEC (Fig. 1b) and are built over the Liquiñe-Ofqui Fault Zone (LOFZ), a major intra-arc structure (ca 1000 km long; Cembrano et al., 2000) that controls the distribution of numerous volcanic edifices in the Southern Volcanic Zone (SVZ) of the Andes (e.g., López-Escobar et al., 1995a; Lara et al., 2006; Cembrano and Lara, 2009). The Caburgua cones are specifically built upon the Late Miocene Trancura granitoids (Moreno and Lara, 2008).

The Caburgua cones and their associated lavas comprise five small (< 0.31 km^3 each; Morgado et al., 2015) basaltic centres (Hickey-Vargas et al., 1989; López-Escobar et al., 1995b; Moreno and Lara, 2008), with heights between 152 and 414 m.a.s.l. and volumes between 0.033 and 0.308 km^3. The associated lava flows (49.88-50.78 SiO_2 wt. %; Morgado et al., 2015) and bombs (51.31 SiO_2 wt. %; Table 1) have basaltic compositions and volumes of up to 0.3 km^3 each (Morgado et al., 2015). The whole-rock composition of the Caburgua cones is similar to all those associated with the SECs of CHSEC (Morgado et al., 2015). The lavas and bombs have variable phenocryst contents (7-14%) in a groundmass with <1% glass. Olivine phenocrysts (Fo_{82-84}) have rims of Fo_{74-77}, and some of them have resorption features. The volcanic bomb considered in this article shows olivines with the same textural features and crystal compositions described by Morgado et al. (2015) for all the CHSEC, in particular for the Caburgua cones. This, and the small size of the eruptive deposit suggest the CAB2-2 bomb is a representative sample compared to nearby lavas. Other phenocryst mineral phases are plagioclase (1-5 vol. %), augites (<1 vol. %), and Cr-spinels (mainly as inclusions in olivines, <1 vol. %).

Olivine and augite phenocrysts and microlites of Caburgua lavas have been analysed to determine their crystallisation conditions, using Loucks's (1996) thermometer and Kohler and Brey´s (1990) barometer (Morgado et al., 2015). Morgado et al. (2015) found that the phenocryst pairs give maximum equilibrium temperatures of ~1,170 °C and pressures between 10.8 and 11.4 ± 1.7 kbar for phenocrysts (deep reservoir). The values of the calculated pressure range are similar to the ~10 kbar (~38 km) inferred for the mantle-crust boundary beneath the arc at these latitudes (e.g., Folguera et al., 2007; Haberland et al., 2009; Dzierma et al., 2012a; 2012b). Thus, Morgado et al. (2015) concluded that a magma reservoir is present at the base of the crust. The same authors also found that syn-eruptive olivine-augite microlite pairs give temperatures between 1,081 and 1,130 ºC. Parallel modelling with MELTS software (Ghiorso and Sack, 1995; Asimow and Ghiorso, 1998) yielded slightly higher syn-eruption temperatures of 1,130 to 1,137 ºC, using the whole-rock composition of a low crystallinity (≤ 10%) sample and attempting to reproduce the observed olivine and plagioclase microlite compositions (for details see Morgado et al., 2015). No minerals attributable to the magma ascent or an intermediate reservoir were identified, with the exception of thin rims formed on olivine (Fo_{74-77}) and plagioclase (An_{45-65}) phenocrysts.

3. Analytical Procedure

Compositional profiles (spacing ~4–7 μm) were measured in 8 olivine crystals (See Supplementary Material) of a bomb from Caburgua (CAB2-2) using an electron microprobe at Leeds Electron Microscopy and Spectroscopy Centre, University of Leeds (JEOL JXA8230). The analytical conditions consisted of an accelerating potential of 20 keV and electron beam current of 40 nA for major elements (Si, Fe, Mg) and 100 nA for minor and trace elements (Al, Ca, Ni, Mn, Ti) with a focused beam. Counting times for major elements were 20 seconds (10 s on peak and 10 s on background) and 60 seconds for minor and trace

elements (30 s on peak and 30 s on background). Higher-resolution Mg-Fe diffusion profiles were obtained through back-scattered electron compositional contrast images, using a Scanning Electron Microscope (SEM) at University of Chile (FEI Quanta 250), quantified with ImageJ® software and calibrated with the electron microprobe analyses (e.g. Morgan et al., 2006; Martin et al., 2008; Hartley et al., 2016). Crystallographic orientations were determined (olivine diffusivity depends on crystallographic orientation) in all olivine crystals using electron back-scatter diffraction (EBSD; Prior et al. 1999) on an FEI Quanta 650 FEGSEM equipped with a Nordlys EBSD camera at the School of Earth and Environment, University of Leeds.

4. Diffusion modelling approach

Diffusion can be described and modelled using Fick's second law (compositional-dependent form of the diffusion equation):

$$\frac{\partial C(x,t)}{\partial t} = \frac{\partial}{\partial x}\left(D\frac{\partial C(x,t)}{\partial x}\right) \qquad \text{Eq. 1}$$

where C is composition, t is time, and D is the diffusion coefficient that is described by an Arrhenian relation (Dohmen and Chakraborty, 2007a, b) and depends on crystallographic orientation, temperature, pressure, composition and oxygen fugacity.

Mg-Fe (inter)diffusion in olivine along the [001] direction is calculated by Eq. 2 (Dohmen and Chakraborty, 2007a, b) for $fO_2 > 10^{-10}$ Pa, and this Mg-Fe diffusivity is about six times faster along either the [100] or [010] directions (Dohmen and Chakraborty, 2007b).

$$\mathrm{D}^{\mathrm{Fe-Mg}}_{\mathrm{olivine}} = 10^{-9.21} \cdot \left(\frac{f_{O_2}}{10^{-7}}\right)^{1/6} \cdot 10^{3\cdot(\mathrm{X_{Fe}}-0.1)} \exp\left(-\frac{201{,}000 + (\mathrm{P} - 10^5)\cdot 7\cdot 10^{-6}}{\mathrm{RT}}\right) \qquad \text{Eq. 2}$$

Eq. 2 (Dohmen and Chakraborty, 2007a; b) describes $D^{Fe-Mg}_{olivine}$, the Mg-Fe (inter)diffusion rate in olivine along the [001] direction ($m^2 s^{-1}$), where X_{Fe} is the mole fraction of fayalite

component, P is pressure (Pa), f_{O_2} is oxygen fugacity (Pa), T is temperature (K) and R is the universal gas constant 8.314 J $mol^{-1}K^{-1}$. We can model the diffusion coefficient for any crystallographic orientation using Philibert's (1991) proposition:

$$D_{trav}^{Fe-Mg} = D_{[100]}^{Fe-Mg} (cos(\alpha))^2 + D_{[010]}^{Fe-Mg} (cos(\beta))^2 + D_{[001]}^{Fe-Mg} (cos(\gamma))^2 \qquad \text{Eq. 3}$$

where α, β and γ are angles between the compositional traverse and the a-, b- and c- axes of the olivine, respectively, where D_a^i denotes the diffusivity of element i parallel to the axis direction a.

Homogenous initial profiles were considered for Mg-Fe interdiffusion modelling because this has been suggested as a good assumption for olivine (e.g., Costa and Chakraborty, 2004; Costa et al., 2008). The results of this modelling are similar to those obtained considering a break in the initial composition < 10 µm from the crystal boundary, as the profiles are asymmetric and are consistent with a dominance of exchange between crystal and melt, rather than an internally isolated "stranded" profile. In this sense, there is little timescale variation between cases considering a thin (< 10 µm) or absent boundary zone (e.g., figure 3).

5. Thermodynamic modelling and thermobarometry

The thermodynamic modelling with MELTS software (Ghiorso and Sack, 1995; Asimow and Ghiorso, 1998) was used to explore the equilibrium crystallisation conditions of the olivine rims (Fo_{74-77}). The whole-rock composition of the studied phenocryst-poor (<10%) bomb (CAB2-2, see Table 1) was considered representative of the initial melt composition. The oxygen fugacity was fixed to that equal to the Ni-NiO (NNO) buffer reaction, which is the same oxygen fugacity conditions as the 1971 eruption of the nearby Villarrica stratovolcano (Morgado et al., 2015). Dissolved water contents were modelled from 0 to 1 wt. %, above which the crystallisation of olivine in the range of interest (Fo_{74-77}) could not be reproduced by MELTS.

Each isobaric cooling model was run with a temperature decreasing in 0.5 ºC steps. Each cooling model was run at successive pressures of 0.5 kbar, to match the pressure conditions. This procedure was followed for different values of dissolved water contents (0, 0.25, 0.5, 0.75, and 1 wt. %), which influence the composition of the modeled olivines in MELTS, and is necessary to generate the observed olivine compositions noted above. The considered pressure range was from 10 kbar (equivalent to ~ 38km depth, pressure of the deep reservoir at the base of the crust) to 1bar (atmospheric pressure), whereas the temperatures considered for modelling were bracketed between 1,170 ºC (temperature of the deep reservoir) and 1,130 ºC (syn-eruptive temperature). By using a variety of P, T conditions alongside varying water content, the whole spectrum of the stability field is covered. Determining the intensive conditions over which the observed composition of olivine rims (Fo_{74-77}) are stable defines the stability field of the rims, corresponding to pressures ≤ 2.6 kbar and temperatures that can span the modelled range, dependent on ambient pressure (Fig. 2, grey field).

6. Magmatic timescales calculation

6.1. Considerations of Mg-Fe interdiffusion modelling in olivine

All the olivine crystals used for diffusion modelling are derived from sample CAB2-2, taken from a poor-crystal (< 10%) volcanic bomb. Selection of crystals for timescales calculation was carried out following the criteria described in Costa et al. (2008) and Shea et al. (2015) (i.e., the biggest crystals, profiles away from the corners, clear concentration plateaus, etc). 2D modelling (i.e. at least two 1D traverse measurements in one crystal plane; Costa et al., 2003) was used for verifying the obtained timescales (see Fig. 3) from individual olivine crystals (Shea et al., 2015), as well as to ensure that the gradients are related to diffusion and not associated with crystal growth (Costa et al., 2008).

Previous studies (e.g., Costa et al., 2008; Costa and Morgan, 2010) have demonstrated that the primary factors affecting the uncertainties associated with timescale determinations using zoning profiles are: (i) the inherent difficulties in obtaining precise measurements of diffusivity; (ii) uncertainties associated with temperature variations (diffusivity varies exponentially with temperature due to the $e^{\frac{-\Delta H}{RT}}$ term), and (iii) the initial and boundary conditions. Particular emphasis should be paid to the determination of the thermodynamic conditions under which the zonation formed, as this is one of the most important problems concerning the estimation of residence times (Rutherford, 2008).

Regarding the diffusivity uncertainties, these are related to uncertainties in the activation energy (-ΔH, in kJ/mol), as determined by Dohmen and Chakraborty (2007a; 2007b). Minimum and maximum values of activation energy were used to calculate bracketing diffusivities for different possible temperatures. Temperatures are considered between two end-members, the hottest temperature was equivalent to that determined for the deep reservoir (~1,170ºC) and the coolest temperature considered was equivalent to the inferred syn-eruptive temperature (1,130ºC). The calculations were performed in each profile considering both temperatures giving a range of timescales (Table 2). The initial profile and boundary conditions uncertainties are explained in Section 4.

6.2. Magmatic residence times in the upper crust

For the sample CAB2-2 in the temperature range of 1,130 – 1,170ºC (syn- and pre-eruptive temperatures, respectively), pressure of ≤ 2.6 kbar (see above) was obtained by MELTS for the growth of olivine rims. A pressure of 1.3 kbar was chosen as an intermediate value in the shallow crust, because pressure has only a minor effect on timescales. Oxygen fugacity buffer was assumed equal to that of the NNO buffer (see section 5). The results of modelling indicate significant differences in the times of olivine rim formation at sample scale. Figure 4

and Table 2 show the range in the calculated timescales, where the shortest timescale of 4.9 days was obtained for a temperature of 1,170ºC (the maximum calculated melt temperature, consistent with MELTS modelling only if the water dissolved in melt is 0 wt.%). By contrast, the maximum residence time for an olivine rim was calculated as 471 days (Fig. 4, Table 2), obtained using a melt temperature of 1,130ºC (syn-eruptive temperatures, consistent with MELTS modelling where water dissolved in the melt was 0.25-0.5 wt %). According to McGee et al. (2017) the samples from the Caburgua cones show little evidence of crustal assimilation, this is consistent with short residence timescales in the upper crust.

7. Discussion

7.1 Concerning transient shallow reservoir and magma ascent

The origin of the zoning patterns is suggested to be variations in intensive conditions at the upper crust rather than magma mixing, because the composition of all cones of CHSEC have a very homogeneous basaltic composition (Morgado et al., 2015) and the absence of enclaves in the studied rocks. If magma mixing took place, the compositions could not have been modified by the replenished magma. The short magma residence times in the upper crust and the low Mg-Fe diffusivity of augite, (Müller et al., 2013), could explain why olivine-augite phenocryst pairs formed in the lower crust deep reservoir (see Section 2) were not re-equilibrated in the shallower reservoir. For the clinopyroxenes of the sample CAB2-2, the Mg-Fe interdiffusivities calculated within the same temperature interval as used for olivine is 2 to 3 orders of magnitude lower than in olivine, equivalent to diffusive lengths in pyroxene of less than 1 µm. This is consistent with the apparent lack of zonation in these crystals.

Despite the Caburgua cones belonging to a short-lived volcanic system supplied by dyke transport of magmas from a deeper source (in the lower crust, see Section 2), the calculated

timescales of olivine rim formation would only represent magma ascent time to the surface from a maximum depth of 6.5 km (equivalent to a pressure of 2.6 kbar) obtained at 1,170 °C for olivine rim formation (according to modelling in MELTS, see Fig. 2). Because the olivine rim formation represents a combination of residence and transport (since the olivine overgrowth), we may utilise the shortest timescale (4.9 days) as a proxy to constrain the maximum average ascent speed (considering the calculated times representing only ascent) from that depth, resulting in 1,327 m/day or ~0.015 m/s.

To determine whether the shortest duration of olivine rim residence (4.9 days) corresponds to the fastest magma ascent speed, it is necessary to assess if that speed would be sufficient to avoid freezing during the magma ascent through the upper crust. For that purpose, relevant properties and parameters of the ascending magma dyke and surrounding rock conditions are necessary to assess if magma could reach the surface before freezing including: melt composition, melt relative and apparent viscosity, physical and thermal properties of the crust, critical rate of magma supply, critical magma ascent speed, P-T conditions of the magma, and the dimension of the magma conduit. To calculate the minimum ascent rate necessary to avoid freezing and to compare this with the ascent rates calculated by diffusion timescales, 10,000 simulations were analysed using the method of Menand et al. (2015) (see the MATLAB® script in Supplementary material for details; the equation was fixed according to Menand, personal communication):

$$Q_c = \frac{9}{8}\left(\frac{C_p\,(T_f - T_{inf})}{L\,(T_0 - T_f)}\right)^{9/4}\left(\frac{\Delta\rho g k^3 H^3}{\mu}\right)^{1/4}\left(\frac{K_c}{\Delta\rho g}\right)^{2/3} \qquad Eq.4$$

where Q_c is the minimum magma supply rate that a dyke needs to propagate over a height H (in this case, 6.5 km) without freezing, L is latent heat of magma, C_p is its specific heat capacity, T_0, T_f, and T_{inf} are initial magma temperature (1,170 ºC), freezing temperature

(following the definitions and values given by Menand et al., 2015, the behaviour of magma is solid-like; in the range of ~900 to 1,100 ºC), and crustal far-field temperature (temperature of the crust horizontally distal from the source of heating; 30-450 ºC) respectively, k is the country-rock thermal diffusivity, $\Delta\rho$ is the density difference between country rock and magma, g is gravitational acceleration (9.8 m/s), and μ is magma dynamic viscosity. Values of L, C_p, k, and $\Delta\rho$ were taken from Menand et al. (2015) and references therein (details of calculation in Supplementary Material).

The minimum magma supply rate (Qc) of ~0.06 km^3/yr for avoiding freezing that was obtained from the aggregate results of 10,000 simulations is higher than the rate associated with magma transfer where olivine rim (shortest) timescales represent only ascent (~0.038 km^3/yr; Fig. 4, Table 2; for all the values and details constraining Qc, see Supplementary Material). Therefore the olivine rims must represent the sum of both the residence time in a reservoir and the ascent time. This is even more evident if residence times given by other olivine crystals are considered, because for explaining the timescales of all measured olivine crystals a Qc lower than ~0.0015 km^3/yr is necessary (Fig.4, Table 2; see crystal CAB2-2 20).

The magma ascent speeds related to each olivine crystal can be calculated considering the distance travelled by the magma during the ascent (6.5 km) and the obtained timescales (in days); then the magma supply rate associated to each crystal (for comparison with Qc value) was calculated considering ascent speed in a cylindrical conduit with a radius of 5 m as a representation of a dyke, following the example of Valentine and Krogh (2006). Although studies of analogue modelling (e.g. Takada, 1990; Rivalta et al., 2005) suggest that magma conduits might be different from a cylinder, cylindrical models are quite prevalent in the literature (e.g., Melnik and Sparks, 1999; 2005; Costa et al., 2007; Vedeneeva, 2007;

Gonnermann and Manga, 2012). Such models are also supported by the field evidence of Valentine and Krogh (2006), who studied multiple centres in the Pauite Ridge volcanic field.

The conditions necessary to avoid freezing during ascent can then be further investigated by considering the equivalent magma ascent speed ~0.015 m/s (related to 4.9 days magmatic ascent; Table 2, Fig. 4b). Thus, data of the minimum magma ascent speed for explosive eruptions at stratovolcanoes (0.2 m/s; from Rutherford, 2008 and references therein) was used for comparison with Caburgua (Fig. 4b). The value given by Rutherford (2008) is higher than the maximum ascent speed calculated using in olivine rims if those timescales only represented ascent, supporting the hypothesis that olivine rims must represent the sum of both the residence time in a reservoir and the ascent time.

Transient reservoirs have also been recognized in other volcanic systems. For example, based on time-dependent seismic tomography (yearly-time windows) in the Klyuchevskoy volcanic group, Koulakov et al. (2013) found short-lived channels and transient reservoirs feeding eruptions. The same authors suggested that stress release would cause the closure of the cracks after the eruption and that neither melts nor fluids would be found in the place where the reservoir (or reservoirs) used to be. Shapiro et al. (2017) have also recognized shallow magma reservoirs in the Klyuchevskoy volcanic group through seismic signals.

7.2. Geological controls on magma residence

The obtained short residence times in the upper crust suggest that Caburgua magma storage and differentiation occurred mainly in the lower crust, probably in a very deep reservoir (32-44 km; Morgado et al., 2015). Several models for arc magma storage have been proposed which are compatible with this inference, such as MASH zones (Melting Assimilation Storage and Homogenization; Hildreth and Moorbath, 1988) and deep crustal hot zones (Annen et al., 2005). Such systems have also been invoked previously to explain the

evolution of magmas associated with small eruptive centres elsewhere in Southern Volcanic Zone (e.g., Bucchi et al., 2015).

Although volcanism is most commonly linked to extensional settings (i.e. magma ascent; Cas and Wright, 1987; Watanabe et al., 1999; Acocella and Korme, 2002), compressive regimes cannot be precluded (Galland et al., 2007; Tibaldi, 2005, 2008). In different systems if magma moves from a medium of low rigidity to one of higher rigidity during its ascent, the rigidity contrast causes magma ascent to decelerate and possibly arrest dyke propagation (Rivalta et al., 2005). Thus, the presence of granitoids (high-rigidity) below the Caburgua cones is plausibly consistent with the hiatuses in magma ascent and the existence of transient reservoirs. Localised extensional settings can be found in transpressive regimes, particularly in the Liquiñe-Ofqui Fault Zone (LOFZ), and they have been associated with volcanic fields displaying short crustal magma residence times over the LOFZ (Cembrano and Lara, 2009) and rapid magma ascent.

7.3. Intervals between eruptions of a monogenetic volcanic field

According to Marsh (1989), in continental magma systems geophysical data indicate that inferred magma chambers have similar sizes to the volume of the erupted material. Further study by White et al., (2006) suggested that the intruded volume may be considered as ~5 times that of the extruded component. To perform an order-of-magnitude estimation of the inter-eruption timescale, we can combine the proposals of Marsh (1989) and White et al. (2006) with the given extruded magma volume in Caburgua of 0.13 km^3 (Morgado et al., 2015) to give a probable intruded volume of ~0.13-0.65 km^3. This can then be considered with the minimum magma input rate R_{min}, of ~0.005 km^3/yr for a viable magma body of a similar size of a few km^3 in volume from the calculations of Gelman et al., (2013), via the relation:

$$t = \frac{V_{int}}{R_{min}} \quad Eq.5$$

where t is time (years), and V_{int} is the annual intruded volume (km^3).

The calculated period would indicate the interval between eruptions of the Caburgua field as a whole, if the magmas passed through a common transient shallow-crustal reservoir assuming only one pause in ascent, within the upper crust. If this magma input rate were valid for Caburgua, then the period between eruptions should be on the order of decades (depending on the ratio of intruded/extruded magma, see Supplementary Material).

Our model for the Caburgua system would consist of a background supply of magma to a deeper magma reservoir at the base of the crust (32-44 km), which is sufficient to occasionally support a transient magma shallow chamber at depths less than 6.5 km. Continued magma transfer from the deep reservoir could sustain the shallow reservoir and enable a series of eruptions at decadal frequencies, before the transient chamber inevitably freezes and the system returns to quiescence. This pattern of infrequent bursts of activity across fields of small eruptive centres is compatible with patterns seen in historical activity such as at the volcanic fields of Carrán-Los Venados (SVZ, Chile). Here, three associated centres: Riñinahue maar, Carrán maar and Mirador cone, all located within 2 km of each other, erupted in 1907, 1955 and 1979, respectively (Moreno, 1980), following a ~150-year hiatus in activity (Pocura maar; Bucchi et al., 2015).

8. Conclusions

The Caburgua cones are examples of small eruptive centres built over the intra-arc transpressive Liquiñe-Ofqui Fault Zone developed along the Andean Southern Volcanic Zone. They erupted material evidence from two reservoirs of different depths in the crust (Fig. 5). A deep reservoir, is located at the mantle-crust boundary (Morgado et al., 2015), and

a shallow-crustal transient reservoir, at a depth equivalent to P ≤ 2.6 kbar (Fig. 2; Fig. 5). Magma residence times in the shallow reservoir of ≤ 471 days were obtained via Mg-Fe diffusional relaxation times of the rim zones of olivine phenocrysts, extracted from a volcanic bomb. Modelling the magma system indicates that magma residence is strongly influenced by the magma input rate necessary to prevent magma freezing, and it is much shorter than the decadal timescale of magma residence predicted for crystals in the shallow reservoir of the nearby Villarrica stratovolcano by the calculations of Lohmar et al. (2012).

This study establishes via crystal-chemical and kinetic timescale studies in olivine the presence of a transient crustal magma body at the Caburgua cones before the eruption. The magma volumetric supply rate and ascent speeds (related to one eruption) calculated to be ≥ 0.06 km^3/yr and (the equivalent) ≥ 0.025 m/s respectively.

The presence of a short-lived transient reservoir could explain why magmas of small eruptive centres are evacuated in bursts of activity over decadal timescales by numerous, neighbouring vents in contrast with the single-vent evacuation of stratovolcanoes, which would have efficiently permanent, larger-volume reservoirs because of higher magma input rates.

Acknowledgments

We acknowledge to Maren Kahl, Richard Walshaw, and Duncan Hedges that provided us assistance with the EBSD at University of Leeds. Fruitful discussion with Martin Reich, Maren Kahl, Nicolas Vinet and Lucy McGee are greatly appreciated. We acknowledge to Thierry Menand for his help in the calculation of the minimum rate of magma supply for avoiding freezing. We thank the help on the field of Gabriela Pedreros and Alejandra Salas. The financial support through FONDAP project 15090013 MSc fellowships (EM and CC) and CONICYT PhD fellowship (72160268, EM) and MSc fellowship (22130368, CC) are acknowledged. EM would like to specially thank to Claire “the amazing” Harnett, Patrick

"the chosen one" Sugden and Ruth Amey. We thank three anonymous reviewers for their detailed and constructive comments. Editorial handling of J. Gardner is greatly appreciated.

References

Acocella, V., Korme, T., 2002. Holocene extension direction along the Main Ethiopian Rift, East Africa, Terra Nova 14 (3), 191–197. doi: http://dx.doi.org/10.1046/j.1365-3121.2002.00403.x

Annen, C., Blundy, J.D., Sparks, R.S.J., 2005. The Genesis of Intermediate and Silicic Magmas in Deep Crustal Hot Zones. J. Petrol. 47(3):505–539. doi: http://dx.doi.org/10.1093/petrology/egi084

Asimow, P.D., Ghiorso, M.S., 1998. Algorithmic modifications extending melts to calculate subsolidus phase relations. Am. Mineral. 83:1127–1131. doi: http://dx.doi.org/0003–004X/98/0910–0000$05.00

Bouvet de Maisonneuve, C., Dungan, M.A., Bachmann, O., Burgisser, A., 2012. Insights into shallow magma storage and crystallization at Volcán Llaima (Andean Southern Volcanic Zone, Chile). J. Volcanol. Geotherm. Res. 211-212:76–91. doi: http://dx.doi.org/10.1016/j.jvolgeores.2011.09.010

Bucchi, F., Lara, L.E., Gutiérrez, F., 2015. The Carrán – Los Venados volcanic field and its relationship with coeval and nearby polygenetic volcanism in an intra-arc setting. J. Volcanol Geotherm. Res. 308:70–81. doi: http://dx.doi.org/10.1016/j.jvolgeores.2015.10.013

Cañón-Tapia, E., Walker, G.P., 2004. Global aspects of volcanism: the perspectives of "plate tectonics" and "volcanic systems". Earth-Sci. Rev. 66(1–2): 163–182. doi: http://dx.doi.org/10.1016/j.earscirev.2003.11.001

Cas, R.A.F., Wright, J.V., 1987. Volcanic Successions, 528 p. Allen and Unwin, St. Leonards, N.S.W., Australia.

Cembrano, J., Hervé, F., Lavenu, A., 1996. The Liquiñe-Ofqui fault zone: a long-lived intra-arc fault system in southern Chile. Tectonophysics 259: 55-66. doi: https://doi.org/10.1016/0040-1951(95)00066-6

Cembrano, J., Lara, L., 2009. The link between volcanism and tectonics in the southern volcanic zone of the Chilean Andes: A review. Tectonophysics 471: 96-113. doi: http://dx.doi.org/10.1016/j.tecto.2009.02.038

Cembrano, J., Schermer, E., Lavenu, A., Sanhueza, A., 2000. Contrasting nature of deformation along an intra-arc shear zone, the Liquiñe – Ofqui fault zone, Southern Chilean Andes. Tectonophysics 319: 129–149. doi: http://dx.doi.org/10.1016/S0040-1951(99)00321-2

Chamberlain, K.J., Morgan, D.J., Wilson, C.J.N., 2014. Timescales of mixing and mobilisation in the Bishop Tuff magma body: Perspectives from diffusion chronometry. Contrib. Mineral. Petr. 168:1-24 doi: http://dx.doi.org/10.1007/s00410-014-1034-2

Condomines, M., Hemond, C., Allegre, C.J., 1988. U-Th-Ra radioactive disequilibria and magmatic processes. Earth. Planet. Sc. Lett. 90, 243-262. doi: http://dx.doi.org/10.1016/0012-821X(88)90129-X

Connor, C.B., Stamatakos, J.A., Ferrill, D.A., Hill, B.E., Ofoegbu, G.I., Conway, F. M., Sagar, B., Trapp, J., 2000. Geologic factors controlling patterns of small-volume basaltic volcanism: Application to a volcanic hazards assessment at Yucca Mountain, Nevada, J Geophys Res 105(1): 417–432. http://dx.doi.org/10.1029/1999JB900353

Cook, C., Briggs, R.M., Smith, I.E.M., Maas, R., 2005. Petrology and Geochemistry of Intraplate Basalts in the South Auckland Volcanic Field, New Zealand : Evidence for Two Coeval Magma Suites from Distinct Sources, J. Petrol. 46(3):473–503. doi: http://dx.doi.org/10.1093/petrology/egh084

Costa, A., Melnik, O., Vedeneeva, E., 2007. Thermal effects during magma ascent in conduits. J. Geophys. Res.: Solid Earth, 112(B12). doi: http://dx.doi.org/10.1029/2007JB004985

Costa, F., Andreastuti, S., Bouvet de Maisonneuve, C., Pallister, J.S., 2013. Petrological insights into the storage conditions, and magmatic processes that yielded the centennial 2010 Merapi explosive eruption. J. Volcanol. Geotherm. Res. 261, 209–235. doi: http://doi.org/10.1016/j.jvolgeores.2012.12.025

Costa, F., Dungan, M., 2005. Short time scales of magmatic assimilation from diffusion modelling of multiple elements in olivine. Geology 33:837-840. doi: http://dx.doi.org/10.1130/G21675.1

Costa, F., Chakraborty, S., 2004. Decadal time gaps between mafic intrusion and silicic eruption obtained from chemical zoning patterns in olivine. Earth Planet. Sci. Lett. 227,517-530. doi: https://doi.org/10.1016/j.epsl.2004.08.011

Costa, F., Chakraborty, S., Dohmen, R., 2003. Diffusion coupling between trace and major elements and a model for calculation of magma residence times using plagioclase. Geochim. Cosmochim. Ac. 67(12):2189-2200. doi: http://dx.doi.org/10.1016/S0016-7037(02)01345-5

Costa, F., Dohmen, R., Chakraborty, S., 2008. Time scales of magmatic processes from modeling the zoning patterns of crystals. Rev. Mineral. Geochem. 69:545–594. doi: http://dx.doi.org/1529-6466/08/0069-0014$05.00

Costa, F., Morgan, D.J., 2010. Timescales of Magmatic Processes, In: Dosseto, A.; Turner, S.; Van-Orman, J. (Ed) Timescales of Magmatic Processes, Wiley-Blackwell.

Dohmen, R., Chakraborty, S., 2007. Fe–Mg diffusion in olivine I: experimental determination between 700 and 1,200 ° C as a function of composition, crystal orientation and oxygen fugacity. Phys. Chem. Miner. 34:389–407. doi: http://dx.doi.org/10.1007/s00269-007-0157-7

Dohmen, R., Chakraborty, S., 2007. Fe–Mg diffusion in olivine II: point defect chemistry, change of diffusion mechanisms and a model for calculation of diffusion coefficients in natural olivine. Phys. Chem. Miner. 34:409–430. doi: http://dx.doi.org/10.1007/s00269-007-0158-6

Dzierma, Y., Thorwart, M., Rabbel, W., 2012a. Moho topography and subducting oceanic slab of the Chilean continental margin in the maximum slip segment of the 1960 Mw 9.5 Valdivia (Chile) earthquake from P-receiver functions. Tectonophysics 530-531:180-192. doi: http://dx.doi.org/10.1016/j.tecto.2011.12.016

Dzierma, Y., Thorwart, M., Rabbel, W., Siegmund, C., Comte, D., Bataille, K., Iglesia, P., Prezzi, C., 2012b. Seismicity near the slip maximum of the 1960 Mw 9.5 Valdivia earthquake (Chile): Plate interface lock and reactivation of the subducted Valdivia Fracture Zone. J Geophys Res 117:B06312. doi: http://dx.doi.org/10.1029/2011JB008914

Endo, E.T., Murray, T.L., Power, J.A., 1996. A comparison of pre-eruption, real-time seismic amplitude measurements for eruptions at Mount St. Helens, Redoubt Volcano, Mount Spurr, and Mount Pinatubo. In: Fire & Mud: eruptions and lahars of Mount Pinatubo, Philippines. Newhall CG, Punongbayan RS (eds) University of Washington Press, Seattle, 233-246.

Folguera, A., Introcaso, A., Giménez, M., Ruiz, F., Martínez, P., Tunstall, C., García Morabito, E., Ramos, V., 2007. Crustal attenuation in the Southern Andean retroarc (38°–39°30′ S) determined from tectonic and gravimetric studies: The Lonco-Luán asthenospheric anomaly. Tectonophysics 439:129-147. doi: http://dx.doi.org/10.1016/j.tecto.2007.04.001

Galland, O., Hallot, E., Cobbold, P.R., Ruffet, G., 2007. Volcanism in a compressional Andean setting : A structural and geochronological study of Tromen volcano (Neuquén province, Argentina). Tectonics 26. doi: http://dx.doi.org/10.1029/2006TC002011

Gelman, S.E., Gutiérrez, F.J., Bachmann, O., 2013. On the longevity of large upper crustal silicic magma reservoirs. Geology, 41(7):759–762. doi: http://dx.doi.org/10.1130/G34241.1

Ghiorso, M.S., Sack, R.O., 1995. Chemical mass transfer in magmatic processes: IV. A revised and internally consistent thermodynamic model for the interpolation and extrapolation of liquid–solid equilibria in magmatic systems at elevated temperatures and pressures. Contrib. Mineral. Petr. 119:197–212. doi: http://dx.doi.org/10.1007/BF00307281

Ginibre, C., Wörner, G., 2007. Variable parent magmas and recharge regimes of the Parinacota magma system (N. Chile) revealed by Fe, Mg and Sr zoning in plagioclase. Lithos 98:118–140. doi: http://dx.doi.org/10.1016/j.lithos.2007.03.004

Gonnermann, H. M., & Manga, M., 2013. Dynamics of magma ascent in the volcanic conduit. In: Fagents, S.A., Gregg, T.K.O., Lopes, R.M.C. (Eds.), Modeling volcanic processes: The physics and mathematics of volcanism. Cambridge University Press, 55-84.

Gutiérrez, F., Gioncada, A., González Ferrán, O., Lahsen, A., Mazzuoli, R., 2005. The Hudson Volcano and surrounding monogenetic centres (Chilean Patagonia): An example of volcanism associated with ridge – trench collision environment. . J. Volcanol. Geotherm. Res. 145:207–233. doi: http://dx.doi.org/10.1016/j.jvolgeores.2005.01.014

Haberland, C., Rietbrock, A., Lange, D., Bataille, K., Hofmann, S., 2009. Interaction between forearc and oceanic plate at the south-central Chilean margin as seen in local seismic data. Geophys. Res. Lett. 33:L23302. doi: http://dx.doi.org/10.1029/2006GL028189

Hartley, M.E., Morgan, D.J., Maclennan, J., Edmonds, M., Thordarson, T., 2016. Tracking timescales of short-term precursors to large basaltic fissure eruptions through Fe–Mg diffusion in olivine. Earth. Planet. Sc. Lett. 439, 58–70. doi: http://dx.doi.org/10.1016/j.epsl.2016.01.018

Hickey-Vargas, R., Moreno, H., López Escobar, L., Frey, F., 1989. Geochemical variations in Andean basaltic and silicic lavas from the Villarrica–Lanín volcanic chain (39.5°S): an evaluation of source heterogeneity, fractional crystallization and crustal assimilation. Contrib. Mineral. Petr. 103, 361–386. doi: http://dx.doi.org/10.1007/BF00402922

Hildreth, W., Moorbath,. S., 1988. Crustal contributions to arc magmatism in the Andes of Central Chile. Contrib. Mineral. Petr. 98:455–489.

Jicha, B. R., Singer, B. S., Beard, B. L., Johnson, C. M., Moreno-Roa, H., Naranjo, J. A., 2007. Rapid magma ascent and generation of 230 Th excesses in the lower crust at Puyehue–Cordón Caulle, Southern Volcanic Zone, Chile. Earth Planet. Sc. Lett. 255(1), 229-242. doi: https://doi.org/10.1016/j.epsl.2006.12.017

Johnson, E.R., Wallace, P.J., Cashman, K.V., Delgado-Granados, H., Kent, A.J.R., 2008. Magmatic volatile contents and degassing-induced crystallization at Volcán Jorullo, Mexico: Implications for melt evolution and the plumbing systems of monogenetic volcanoes. Earth Planet. Sc. Lett. 269:478-487. doi: http://dx.doi.org/10.1016/j.epsl.2008.03.004

Kahl, M., Chakraborty, S., Costa, F., Pompilio, M., 2011. Dynamic plumbing system beneath volcanoes revealed by kinetic modeling, and the connection to monitoring data: An example from Mt. Etna. Earth Planet. Sc. Lett. 308:11-22. doi: http://dx.doi.org/10.1016/j.epsl.2011.05.008

Kahl, M., Chakraborty, S., Pompilio, M., Costa, F., 2015. Constraints on the Nature and Evolution of the Magma Plumbing System of Mt. Etna Volcano (1991 – 2008) from a Combined Thermodynamic and Kinetic Modelling of the Compositional Record of Minerals. J. Petrol., 56(10), 2025–2068. doi: http://doi.org/10.1093/petrology/egv063

Kahl, M., Chakraborty, S., Costa, F., Pompilio, M., Liuzzo, M., Viccaro, M., 2013. Compositionally zoned crystals and real-time degassing data reveal changes in magma transfer dynamics during the 2006 summit eruptive episodes of Mt. Etna. B. Volcanol. 75:692. doi: http://dx.doi.org/10.1007/s00445-013-0692-7

Kahl, M., Viccaro, M., Ubide, T., Morgan, D.J., Dingwell, D.B., 2017. A Branched Magma Feeder System during the 1669 Eruption of Mt. Etna: Evidence from a Time-integrated Study of Zoned Olivine Phenocryst Populations. J. Petrol., 58(3), 443–472. doi: http://doi.org/10.1093/petrology/egx022

Köhler, T.P., Brey, G.P., 1990. Calcium exchange between olivine and clinopyroxene and clinopyroxene calibrated as a geothermobarometer for natural peridotites from 2 to 60 kb

with applications. Geochim. Cosmochim. Ac. 54:2375-2388. doi: http://dx.doi.org/10.1016/0016-7037(90)90226-B

Koulakov, I., Gordeev, E.I., Dobretsov, N.L., Vernikovsky, V.A., Senyukov, S., Jakovlev, A., Jaxybulatov, K., 2013. Rapid changes in magma storage beneath the Klyuchevskoy group of volcanoes inferred from time-dependent seismic tomography. J. Volcanol. Geotherm. Res. 263, 75–91. doi: http://doi.org/10.1016/j.jvolgeores.2012.10.014

Lara, L., Lavenu, A., Cembrano, J., Rodríguez, C., 2006. Structural controls of volcanism in transversal chains: Resheared faults and neotectonics in the Cordón Caulle–Puyehue area (40.5°S), Southern Andes. J. Volcanol. Geotherm. Res. 158:70-86. doi: http://dx.doi.org/10.1016/j.jvolgeores.2006.04.017

Lees, J.M., Crosson, R.S., 1989. Tomographic inversion for three-dimensional velocity structure at Mount St. Helens using earthquake data. J. Geophys. Res. 94:5716-5728. doi: http://dx.doi.org/10.1029/JB094iB05p05716

Lohmar, S., Parada, M.A., Gutiérrez, F., Robin, C., Gerbe, M.C., 2012. Mineralogical and numerical approaches to establish the pre-eruptive conditions of the mafic Licán Ignimbrite, Villarrica Volcano (Chilean Southern Andes). J. Volcanol. Geotherm. Res. 235-236:55-69. doi: http://dx.doi.org/10.1016/j.jvolgeores.2012.05.006

López-Escobar, L., Parada, M.A., Hickey-Vargas, R., Frey, F.A., Kempton, P.D., Moreno, H., 1995a. Calbuco Volcano and minor eruptive centers distributed along the Liquiñe-Ofqui Fault Zone, Chile (41º-42º S): contrasting origin of andesitic and basaltic magma in the Southern Volcanic Zone of the Andes. Contrib. Mineral. Petr. 119:345-36. doi: http://dx.doi.org/10.1007/BF00286934

López-Escobar L., Cembrano J., Moreno, H., 1995b. Geochemistry and tectonics of the Chilean Southern Andes basaltic quaternary volcanism (37–46°S). Rev. Geol. Chile. 22(2):219–234.

Loucks, R., 1996. A precise olivine–augite Mg–Fe-exchange geothermometer. Contrib. Mineral. Petr. 125:140–150. doi: http://dx.doi.org/10.1007/s004100050211

Luhr, J.F., Carmichael I.S.E., 1985. Jorullo Volcano, Michoacfin, Mexico (1759-1774): The earliest stages of fractionation in calc-alkaline magmas. Contrib. Mineral. Petr. 90:142–161. doi: http://dx.doi.org/10.1007/BF00378256

Martin, V.M., Morgan, D.J., Jerram, D.A., Caddick, M.J., Prior, D.J., Davidson, J.P., 2008. Bang! Month-Scale Eruption Triggering at Santorini Volcano. Science 321:1178. doi: http://dx.doi.org/10.1126/science.1159584

Marsh, B.D., 1989. Magma chambers. Ann. Rev. Earth Planet. Sci. 17: 439-474.

Mcgee, L.E., Brahm, R., Rowe, M.C., Handley, H.K., Morgado, E., Lara, L.E., Turner, M.B., Vinet, N., Parada, M.Á., Valdivia, P., 2017. A geochemical approach to distinguishing competing tectono - magmatic processes preserved in small eruptive centres. Contrib. Mineral. Petr. 172(6), 1–26. doi: http://doi.org/10.1007/s00410-017-1360-2

McGee, L.E., Millet, M-A., Smith, I.E.M., Németh, K., Lindsay, J.M., 2012. The inception and progression of melting in a monogenetic eruption: Motukorea volcano, the Auckland Volcanic Field, New Zealand. Lithos 155(0): 360–374. doi: http://dx.doi.org/10.1016/j.lithos.2012.09.012

Mcgee, L.E., Smith, I.E.M., 2016. Interpreting chemical compositions of small scale basaltic systems : A review. J. Volcanol. Geotherm. Res. 325: 45–60. doi: http://dx.doi.org/10.1016/j.jvolgeores.2016.06.007

Melnik, O., Sparks, R.S.J., 1999. Nonlinear dynamics of lava dome extrusion. Nature, 402(6757), 37. doi: http://dx.doi.org/10.1038/46950

Melnik, O., Sparks, R.S.J., 2005. Controls on conduit magma flow dynamics during lava dome building eruptions. J. Geophys. Res.: Solid Earth, 110(B2). doi: http://dx.doi.org/10.1029/2004JB003183

Menand, T., Annen, C., de Saint Blanquat, M., 2015. Rates of magma transfer in the crust: Insights into magma reservoir recharge and pluton growth. Geology 43:199-202. doi: http://dx.doi.org/10.1130/G36224.1

Moreno, H., 1980. La erupción del Volcán Mirador en Abril-Mayo de 1979, Lago Ranco-Riñinahue, Andes del Sur. Universidad de Chile, Departamento de Geología, Comunicaciones N°28, p, 1-23.

Moreno, H., Lara, L., 2008. Geología del área Pucón-Curarrehue, regiones de La Araucanía y De Los Ríos. Servicio Nacional de Geología y Minería, Carta Geológica de Chile, Serie Geológica Básica. No. 115, Mapa Escala 1:100.000.

Morgado, E., Parada, M.A., Contreras, C., Castruccio, A., Gutiérrez, F., McGee, L., 2015. Contrasting records from mantle to surface of two nearby arc volcanic complexes: Caburgua-Huelemolle Small Eruptive Centers and Villarrica Volcano**.** J. Volcanol. Geotherm. Res. 306:1-16. doi: http://dx.doi.org/10.1016/j.jvolgeores.2015.09.023

Morgan, D.J., Blake, S., 2006. Magmatic residence times of zoned phenocrysts: introduction and application of the binary element diffusion modelling (BEDM) technique. Contrib. Mineral. Petr. 151:58-70. doi: http://dx.doi.org/10.1007/s00410-005-0045-4

Morgan, D.J., Blake, S., Rogers, N.W., DeVivo, B., Rolandi, G., Davidson, J.P., 2006. Magma chamber recharge at Vesuvius in the century prior to the eruption of A.D. 79. Geology 34(10): 845–848. doi: http://dx.doi.org/10.1130/G22604.1

Morgan, D.J., Blake, S., Rogers, N.W., DeVivo, B., Rolandi, G., Macdonald, R., Hawkesworth, C.J., 2004. Time scales of crystal residence and magma chamber volume from modeling of diffusion profiles in phenocrysts: Vesuvius 1944. Earth Planet. Sc. Lett. 222(3-4):933–946. doi: http://dx.doi.org/10.1016/j.epsl.2004.03.030

Müller, T., Dohmen, R., Becker, H.W., ter Heege, J.H., Chakraborty, S., 2013. Fe-Mg interdiffusion rates in clinopyroxene: Experimental data and implications for Fe-Mg

exchange geothermometers. Contrib. Mineral. Petr. 166(6):1563–1576. doi: http://dx.doi.org/10.1007/s00410-013-0941-y

Németh, K., 2010. Monogenetic volcanic fields: Origin, sedimentary record, and relationship with polygenetic volcanism. In: Cañón-Tapia, E., Szakács, A., (Eds.), What is a volcano?: Geological Society of America Special Paper 470, 43-66.

Philibert, J., 1991. Atom Movements, Diffusion and Mass Transport in Solids, Les éditions de Physique, Les Ulis, France, p. 577.

Prior, D.J., Boyle, A.P., Brenker, F., Cheadle, M.C., Day, A., López, G., Peruzzio, L., Potts, G.J., Reddy, S., Spiess, R., Timms, N.E., Trimby, P., Wheeler, J., Zetterström, L., 1999. The application of electron backscatter diffraction and orientation contrast imaging in the SEM to textural problems in rocks. Am. Mineral. 84:1741–1759. doi: http://dx.doi.org/0003-004X/99/1112–1741$05.00

Rae, A.S.P., Edmonds, M., Maclennan, J., Morgan, D., Houghton, B., Hartley, M.E., Sides, I., 2016. Time scales of magma transport and mixing at Kīlauea Volcano, Hawai'i, Geology 44(6), 463–466. doi: http://doi.org/10.1130/G37800.1

Rivalta, E., Böttinger, M., Dahm, T., 2005. Buoyancy-driven fracture ascent: Experiments in layered gelatine, J. Volcanol. Geotherm. Res. 144: 273–285. doi: http://dx.doi.org/10.1016/j.jvolgeores.2004.11.030

Ruprecht, P., Bachmann, O., 2010. Pre-eruptive reheating during magma mixing at Quizapu volcano and the implications for the explosiveness of silicic arc volcanoes. Geology 10:919–922. doi: http://dx.doi.org/10.1130/G31110.1

Rutherford, M.J., 2008. Magma Ascent Rates. Rev. Mineral. Geochem. 69:241-271. doi: http://dx.doi.org/10.2138/rmg.2008.69.7

Rutherford, M.J., Hill, P.M., 1993. Magma ascent rates from amphibole breakdown: Experiments and the 1980-1986 Mount St. Helens eruptions. J. Geophys. Res. 98:19667-19685. doi: http://dx.doi.org/10.1029/93JB01613

Scandone, R.S., Malone, S., 1985. Magma supply, magma discharge and readjustment of the feeding system of Mount St. Helens during 1980. J. Volcanol. Geotherm. Res. 23(3-4):239-262. doi: http://dx.doi.org/10.1016/0377-0273(85)90036-8

Shapiro, N.M., Droznin, D.V., Droznina, S.Y., Senyukov, S.L., Gusev, A.A., Gordeev, E.I., 2017. Deep and shallow long-period volcanic seismicity linked by fluid-pressure transfer. Nat. Geosci. 10, 442–446. doi: http://doi.org/10.1038/NGEO2952

Shea, T., Costa, F., Krimer, D., Hammer, J.E., 2015. Accuracy of timescales retrieved from diffusion modeling in olivine: A 3D perspective. Am. Mineral. 100(10):2026–2042. doi: http://dx.doi.org/10.2138/am-2015-5163

Smith, I.E.M., Blake, S., Wilson, C.J.N., Houghton, B.F., 2008. Deep-seated fractionation during the rise of a small-volume basalt magma batch: Crater Hill, Auckland, New Zealand. Contrib. Mineral. Petr. 155:511-527. doi: http://dx.doi.org/10.1007/s00410-007-0255-z

Sparks, R.S.J., Baker, L., Brown, R.J., Field, M., Schumacher, J., Stripp, G., Walters, A., 2006. Dynamical constraints on kimberlitic volcanism. J. Volcanol. Geotherm. Res. 155:18-48. doi: http://dx.doi.org/10.1016/j.jvolgeores.2006.02.010

Spera, F.J., 1984. Carbon dioxide in petrogenesis III: role of volatiles in the ascent of alkaline magma with special reference to xenolith-bearing magmas. Contrib. Mineral. Petr. 88:217-232. doi: http://dx.doi.org/10.1007/BF00380167

Takada, A., 1990. Experimental Study on Propagation of Liquid-Filled Crack in Gelatin: Shape and Velocity in Hydrostatic Stress Condition, J. Geophys. Res. 95: 8471–8481.

Takada, A., 1994a. The influence of regional stress and magmatic input on styles of monogenetic and polygenetic volcanism. J. Volcanol. Geotherm. Res. 99: 13563–13573. doi: http://dx.doi.org/10.1029/94JB00494

Takada, A., 1994b. Development of a subvolcanic structure by the interaction of liquid-filled cracks. J. Volcanol. Geotherm. Res. 61(3–4), 207–224. doi: http://dx.doi.org/10.1016/0377-0273(94)90004-3

Tibaldi, A., 2005. Volcanism in compressional tectonic settings : Is it possible? Geophys. Res. Lett. 32:1–4. doi: http://dx.doi.org/10.1029/2004GL021798

Tibaldi, A., 2008. Contractional tectonics and magma paths in volcanoes. J. Volcanol. Geotherm. Res. 176:291–301. doi: http://dx.doi.org/10.1016/j.jvolgeores.2008.04.008

Valentine, G.A., Gregg, T.K.P., 2008. Continental basaltic volcanoes - Processes and problems. J. Volcanol. Geotherm. Res. 177(4): 857-873 doi: http://dx.doi.org/10.1016/j.jvolgeores.2008.01.050

Valentine, G.A., Krogh, K.E.C., 2006. Emplacement of shallow dikes and sills beneath a small basaltic volcanic center – The role of pre-existing structure, Earth Planet. Sc. Lett. 246:217–230. doi: http://dx.doi.org/10.1016/j.epsl.2006.04.031

Valentine, G.A., Perry, F.V., 2007. Tectonically controlled, time-predictable basaltic volcanism from a lithospheric mantle source (central Basin and Range Province, USA). Earth Planet. Sc. Lett. 261: 201-216, doi: http://dx.doi.org/10.1016/j.epsl.2007.06.029

Watanabe, T., Koyaguchi, T., Seno, T., 1999. Tectonic stress controls on ascent and emplacement of magmas. J. Volcanol. Geotherm. Res. 91:65–78. doi: http://dx.doi.org/10.1016/S0377-0273(99)00054-2

Vedeneeva, E.A., 2007. Two-dimensional models of magma flows in a volcanic conduit taking the magma compressibility and thermal effects into account. Fluid Dynam. 42(4), 528-539. doi: https://doi.org/10.1134/S0015462807040035

White, S.M., Crisp, J.A., Spera, F.J., 2006. Long-term volumetric eruption rates and magma budgets. Geochem. Geophy. Geosy. 7(3). doi: http://dx.doi.org/10.1029/2005GC001002

Zellmer, G.F., Blake, S., Vance, D., Hawkesworth, C., Turner, S., 1999. Plagioclase residence times at two island arc volcanoes (Kameni islands, Santorini and Soufriere, St. Vincent) determined by Sr diffusion systematics. Contrib. Mineral. Petr. 136:345–357. doi: http://dx.doi.org/10.1007/s004100050543

Figure 1. a) Location of Caburgua-Huelemolle Small Eruptive Centres (CHSEC) with respect to Chile. b) Geodynamic context of the Caburgua cones. They are located over the LOFZ: Liquiñe-Ofqui Fault Zone (black dashed line; Cembrano et al., 1996) a few km NE from Villarrica stratovolcano (white dashed line represents NW alignment of stratovolcanoes). c) Local-scale distribution of the Caburgua cones and neighbouring small eruptive centres, black lines represent the alignments coinciding with the regional structures in figure 1b (NS and NE described by Cembrano and Lara, 2009).

Figure 2. Calculated stability field of olivine rims (Fo_{74-77}) obtained by MELTS (equilibrium crystallisation) from the composition of the sample CAB2-2 (see Table 1) considering a maximum range of temperatures between 1,170 and 1,130 °C at NNO buffer conditions, and 0 to 1 wt. % of water dissolved.

Figure 3. Example of olivine phenocryst micro-analytical profiles plus associated timescales. a) Backscatter electron (BSE) image of an olivine phenocryst of a bomb erupted from the Caburgua cones (sample CAB2-2), and location of the micro-analytical profiles (traverses 1 and 2) shown in b) and c). b) Forsterite content (Fo = 100*Mg/(Mg+Fe), in mol) measured by electron microprobe corresponding to traverse 1 (trav 1). Circumferences: measured forsterite content; continuous line: best fit diffusion model (highest coefficient of determination, r^2); dashed line: initial forsterite profile. Numbers in days indicate diffusive timescales obtained from best fit model solutions for 1,170 and 1,130ºC. c) Forsterite content calculated from BSE grayscale calibrated profile corresponding to traverse 2 (trav 2). Semi-transparent line: BSE forsterite profile; solid dark line: best fit diffusion model (highest coefficient of determination, r^2); dashed line: initial forsterite profile. Numbers in days indicate diffusive timescales obtained from best fit model solutions for 1,170 and 1,130ºC. d) Plot representing the coefficient of determination (r^2) between BSE profile and the forsterite content measured

in traverse 1. e) Crystallographic orientation (axis a, b, and c) and traverse directions projected onto the stereographic lower hemisphere.

Figure 4. Plots of modelled timescales from Mg-Fe diffusion in 8 olivine crystals. Each horizontal black line represents one calculated crystal timescale (related to a rate of magma supply in "a)" and ascent speed in "b)"). Vertical dashed grey line represents the minimum ascent rate/speed for avoiding freezing according to Menand's et al. (2015) considering a 5 m radius dyke from 6.5 km depth (see Table 2). Vertical continuous line represents the minimum explosive ascent speed in stratovolcanoes according to Rutherford (2008) and references therein.

Figure 5. Schematic representation of the depths of the reservoirs associated to the Caburgua cones (not to scale). The studied volcanic complex would have at least one deep reservoir in the lower crust and a transient shallow reservoir in the upper crust (≤ 6.5 km), where the magmatic residence time is short (≤ 471 days). In the shallow reservoir, the changes of intensive conditions (mainly changes of pressure and likely changes in temperature) can explain the zonation patterns. Then other processes (e.g., magma mixing) are not necessaries.

Table 1. Whole-rock composition of the sample CAB2-2.

Oxide	wt. %
SiO2	51.31
TiO2	1.13
Al2O3	17.45
FeOtot*	9.7
MnO	0.156
MgO	7.45
NiO*	0.01
CoO*	0.004
CaO	8.84
Na2O	3.33
K2O	0.75
P2O5	0.33
total	100.46

All this data were published in Morgado et al. (2015), except where * indicates.

Table 2. Timescales calculated in olivine crystals in two dimensions (two independent profiles: profile 1 based on EPMA data, profile 2 based on BSE images) to give reliability. The rates of magma supply (rates of magma transfer) and magma ascent speed associated with those calculated timescales are also presented.

Crystal	Temperature (ºC)	Profile	Time (days)	Rate of magma supply (km^3/yr)	Ascent speed (m/s)	Profile	Time (days)	Rate of magma supply (km^3/yr)	Ascent speed (m/s)
CAB22-2	1170	1	40.4	0.00461	0.0019	2	42.1	0.00443	0.0018
	1130	1	304.2	0.00061	0.0002	2	315.2	0.00059	0.0002
CAB22-4	1170	1	9.3	0.02004	0.0081	2	8.6	0.02167	0.0087
	1130	1	69.3	0.00269	0.0011	2	64.6	0.00288	0.0012
CAB22-7	1170	1	26.9	0.00693	0.0028	2	18.6	0.01002	0.0040
	1130	1	202.3	0.00092	0.0004	2	140.6	0.00133	0.0005
CAB22-20	1170	1	69.5	0.00268	0.0011	2	51.1	0.00365	0.0015
	1130	1	471.2	0.0004	0.0002	2	385	0.00048	0.0002
CAB22-21	1170	1	5.9	0.03158	0.0128	2	4.9	0.03803	0.0154
	1130	1	44	0.00423	0.0017	2	36.1	0.00516	0.0021
CAB22-23	1170	1	47.9	0.00389	0.0016	2	55.5	0.00336	0.0014
	1130	1	361.3	0.00052	0.0002	2	418.8	0.00044	0.0002
CAB22-25	1170	1	17.8	0.01047	0.0042	2	17	0.01096	0.0044
	1130	1	133.7	0.00139	0.0006	2	127.6	0.00146	0.0006
CAB22-26	1170	1	14.5	0.01285	0.0052	2	6	0.03106	0.0125
	1130	1	55.9	0.00333	0.0013	2	39.1	0.00477	0.0019

* The rate of magma supply was calculated considering a cylindrical conduit of 5 m radius (for an example in nature, see Valentine and Krogh, 2006)

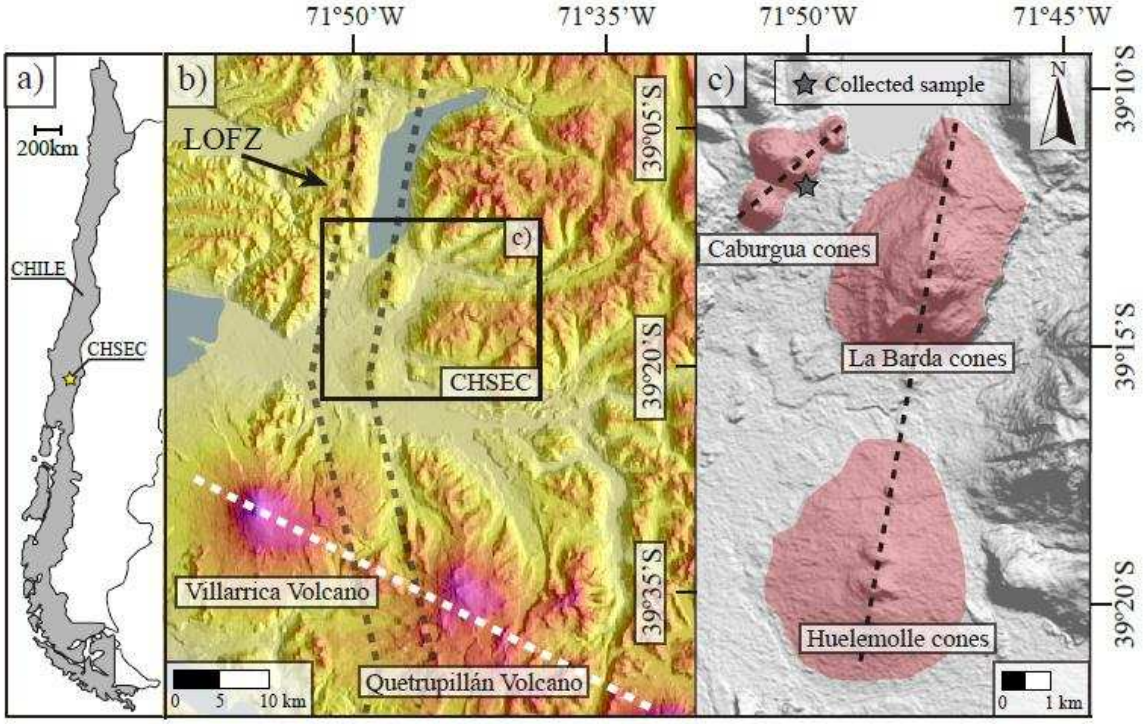

Fig. 1

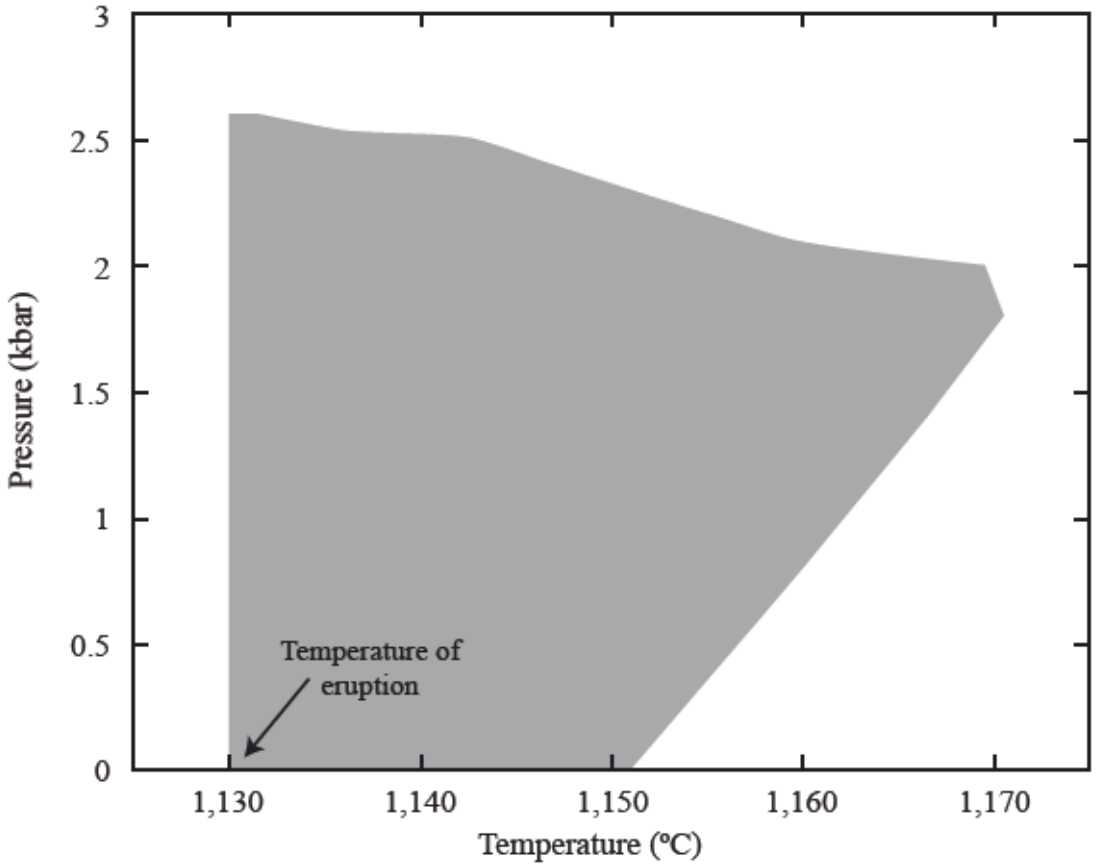

Fig. 2

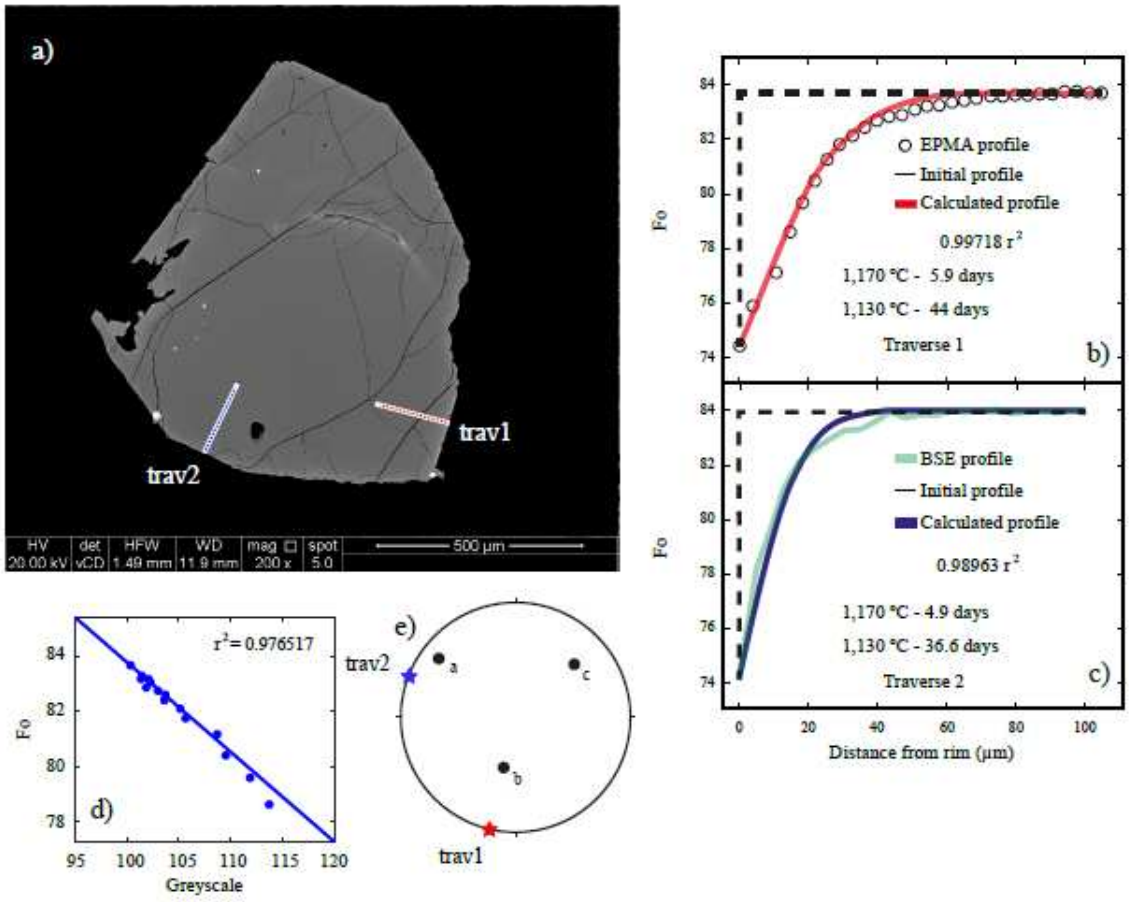

Fig. 3

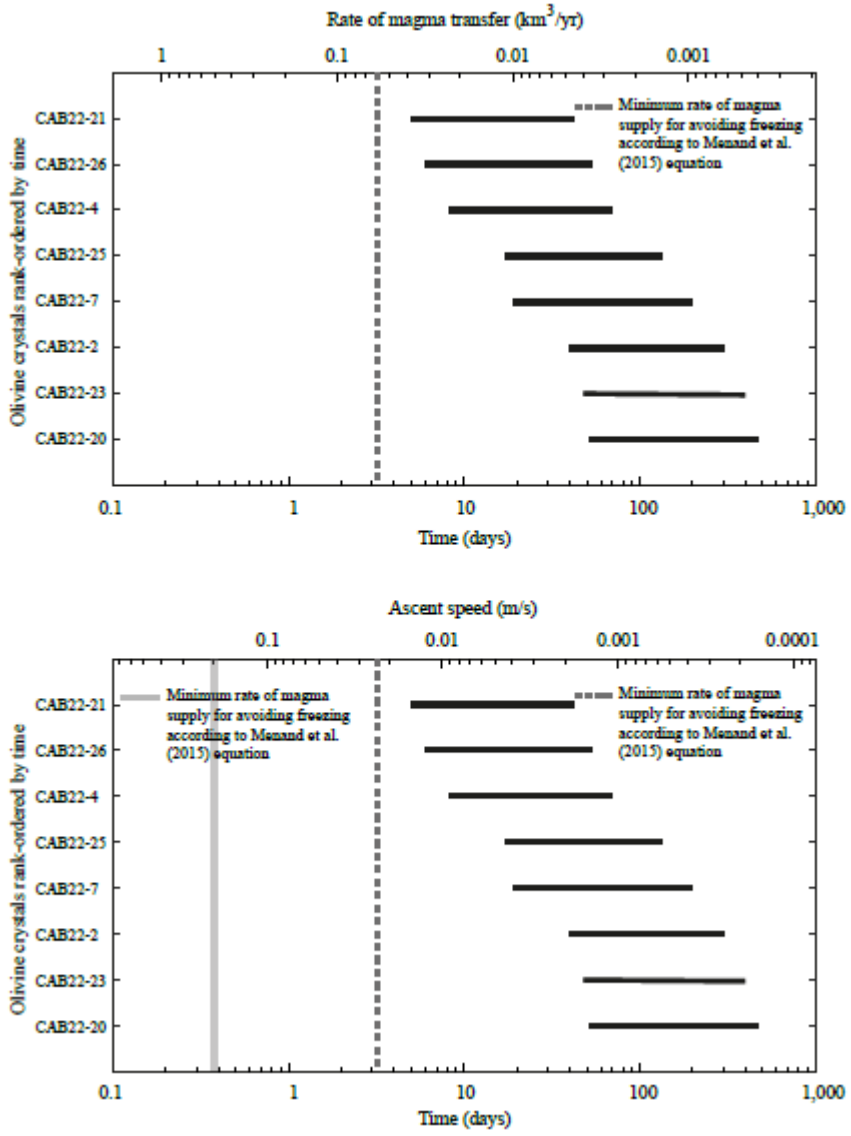

Fig. 4

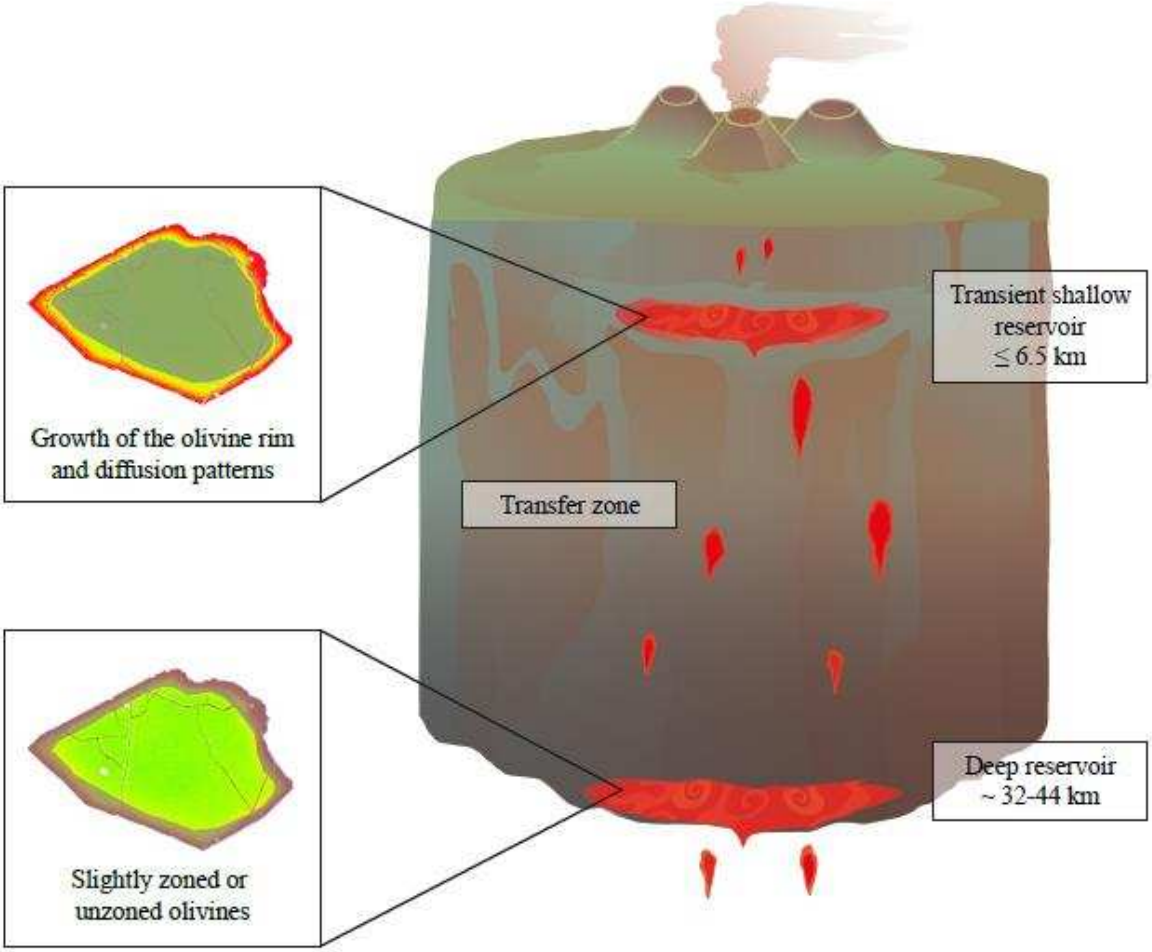

Fig. 5

Highlights:

- Magmatic timescales were calculated from Mg-Fe interdiffusion in olivine.
- The existence is a transient reservoir is deduced from numerical modelling.
- Both minimum ascent speed (~0.02 m/s) and minimum transfer rate (~0.06 km^3/yr) of magma were calculated.
- The longest durations of magma residence seen in the olivine rim zones are up to 229 days.